Spatiotemporal Dynamics

Mark Paul, Keng-Hwee Chiam, Janet Scheel and Michael Cross (Caltech)
Henry Greenside and Anand Jayaraman (Duke)
Paul Fischer (ANL)

Support: Department of Energy, Caltech CACR, NCSC, ANL

Introduction

- Rayleigh-Bénard convection
- Spectral element numerical solution

Spatiotemporal Dynamics

- Chaos in small aspect ratio cryogenic liquid helium
- Mean flow and spiral defect chaos
- Pattern coarsening far from equilibrium
- Rotating convection
- *Travelling waves in rotating annuli*
- *Passive scalar transport in spatiotemporal chaos*
- *Growth of linearized perturbations in spiral defect chaos*

Rayleigh-Bénard Convection

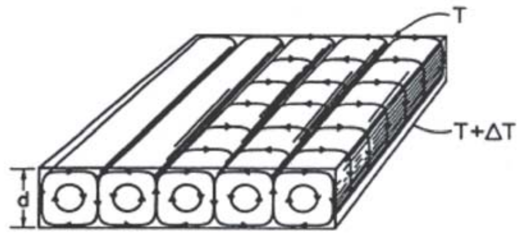

RBC allows a *quantitative* comparison to be made between theory and experiment.

Spatiotemporal Chaos in Large Aspect Ratio Systems

RBC is a rare physical system exhibiting spatiotemporal chaos where numerics and experiments are possible

Many challenges:

- How to characterize it?
  - Sensitive dependence upon initial conditions
  - Low dimensional chaos $\rightarrow$ high dimensional chaos
  - Correlation lengths and times, fractal dimensions
- Can STC be controlled?
- Do large STC systems have properties equivalent to equilibrium systems?
- What is the transition like between chaotic states?

Nondimensional Boussinesq Equations

- Momentum Conservation

$$\frac{1}{\sigma}\left[\frac{\partial \vec{u}}{\partial t} + \left(\vec{u} \bullet \vec{\nabla}\right)\vec{u}\right] = -\vec{\nabla} p + R\, T\hat{e}_z + \nabla^2 \vec{u} + 2\Omega \hat{e}_z \times \vec{u}$$

- Energy Conservation

$$\frac{\partial T}{\partial t} + \left(\vec{u} \bullet \vec{\nabla}\right) T = \nabla^2 T$$

- Mass Conservation

$$\vec{\nabla} \bullet \vec{u} = 0$$

Aspect Ratio: $\Gamma = \frac{r}{h}$

BC: no-slip, insulating or conducting, and constant ΔT

Spectral Element Numerical Solution

- Efficient parallel algorithm
- *Unstructured* mesh generation allows any geometry
  - ◇ Cylindrical geometries possible that avoid singularity in center of domain
- Allows simulation of realistic scenarios
  - ◇ *Rotating* convection
  - ◇ Realistic boundary conditions such as *paper fins* and spatial *ramps* of layer height
  - ◇ *Elliptically* shaped domains
  - ◇ Plan to include thermal sidewalls

[Fischer, J. Comp. Phys. **133** 84 (1997)]

Simulation versus Experiment - Advantages

- Much smaller "noise"
- Complete knowledge of the physical quantities in all three dimensions
  - ◇ Visualization and quantification of the mean flow
- Ability to explore difficult parameter regimes
  - ◇ Very small σ
  - ◇ *Rotating annuli*
  - ◇ Variable geometries
  - ◇ Cylindrical domains of arbitrary aspect ratio, Γ
- Diagnostics available such as the calculation of Lyapunov Exponents

Simulation versus Experiment - Disadvantages

- Simulations can be very expensive even for a highly optimized parallel code
  - ◇ Large aspect ratios
  - ◇ Long time scales, $\tau_h \sim \Gamma^2$
  - ◇ Large Rayleigh numbers, rotation rates, Prandtl numbers
- Analysis can involve large amounts of data
- There are always the issues of time stepping and discretization errors

Chaos in cryogenic liquid helium

- Ahlers in 1974 was one of the first to demonstrate that chaos can occur in a continuous medium like a fluid
- Several aspects of this experiment remained poorly understood (flow visualization was not possible)
- *Power spectra* of $N(t)$ exhibited a power-law dependence $P \sim \omega^{-4}$

Stochastic noise	$?\Longleftrightarrow?$	power law decay
Deterministic chaos	$?\Longleftrightarrow?$	exponential decay

[Ahlers, Phys. Rev. Lett. **33**, 1185 (1974)
Libchaber and Maurer, J. Physique **39**, 369 (1978)
Gao and Behringer, Phys. Rev. A **30**, 2837 (1984)
Pocheau, Croquette, and Le Gal, Phys. Rev. Lett. **55**, 1094 (1985)
Greenside, Ahlers, Hohenberg and Walden, Physica D **322** (1982)]

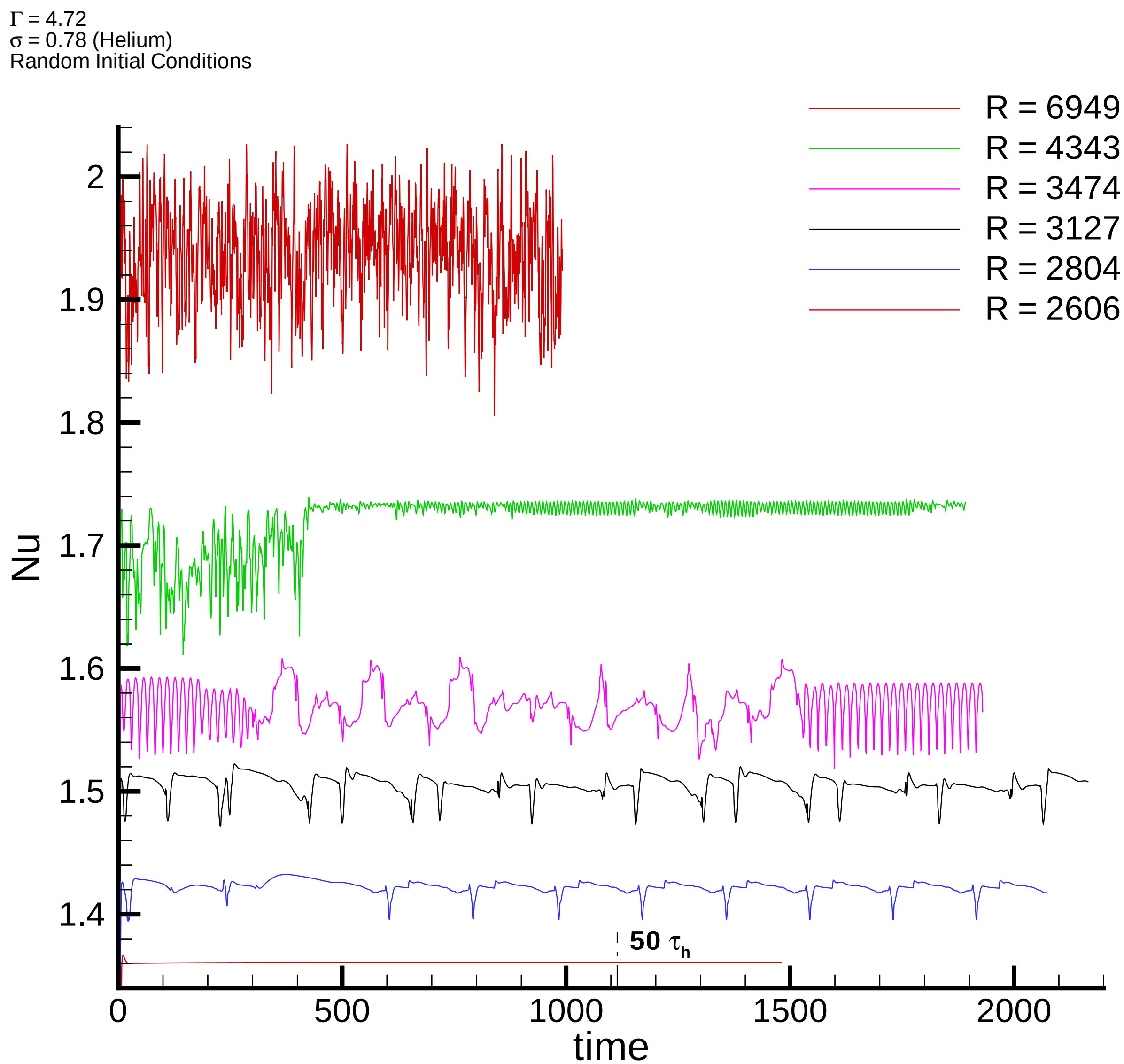
Γ = 4.72
σ = 0.78 (Helium)
Random Initial Conditions
R = 6949
R = 4343
R = 3474
R = 3127
R = 2804
R = 2606
Nu
2
1.9
1.8
1.7
1.6
1.5
1.4
50 τ_h
0
500
1000
1500
2000
time

$R = 2804$ $R = 6949$

Chaos in cryogenic liquid helium

- Simulation exhibits a *power law* over the range accessible to experiment
- When *larger frequencies* are considered an *exponential tail* is found
- Exponential tail not seen in experiment because of instrumental noise floor
- Periodic dynamics also exhibit power-law behavior followed by an exponential tail
- Using the $N(t)$ as a guide, the characteristic *events* are determined to be dislocation nucleation and annihilation from flow *visualizations*
- The power law fall off is seen to be generated during roll pinch-off events (dislocation nucleation and annihilation for the periodic dynamics)

Chaos in cryogenic liquid helium

- The broad plateau of the power spectrum at low frequencies (the chaos) is due to the aperiodic nature of the roll pinch-off events
- The asymptotic power-law behavior of the power spectrum is a consequence of the brief discrete roll pinch-off events
  - This has nothing to do with chaotic dynamics!
- At even higher frequencies (unaccessible in experiment because of the noise floor) we confirmed the exponential decay of the power spectrum as expected for deterministic dynamics
- This showed that Ahlers experiment is consistent with a deterministic chaos description

[Paul, Cross, Fischer, and Greenside Phys. Rev. Lett. **87** 154501 (2001)]

Mean flow and spiral defect chaos

What is mean flow?

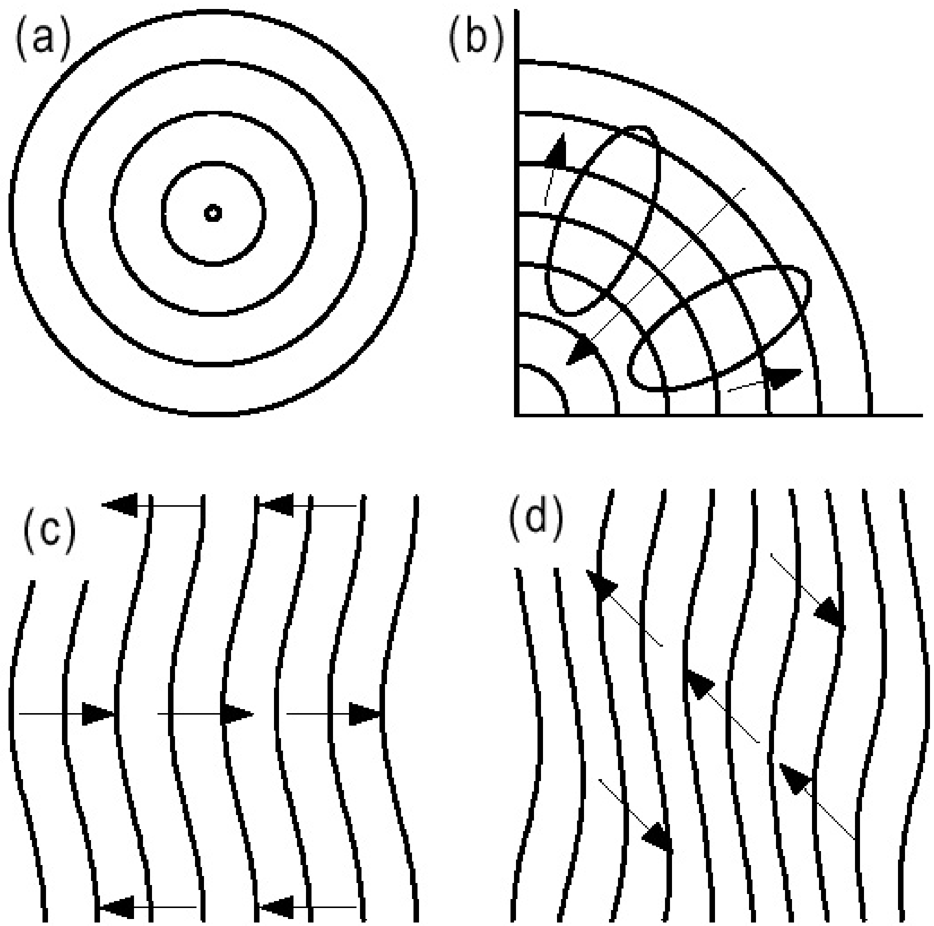

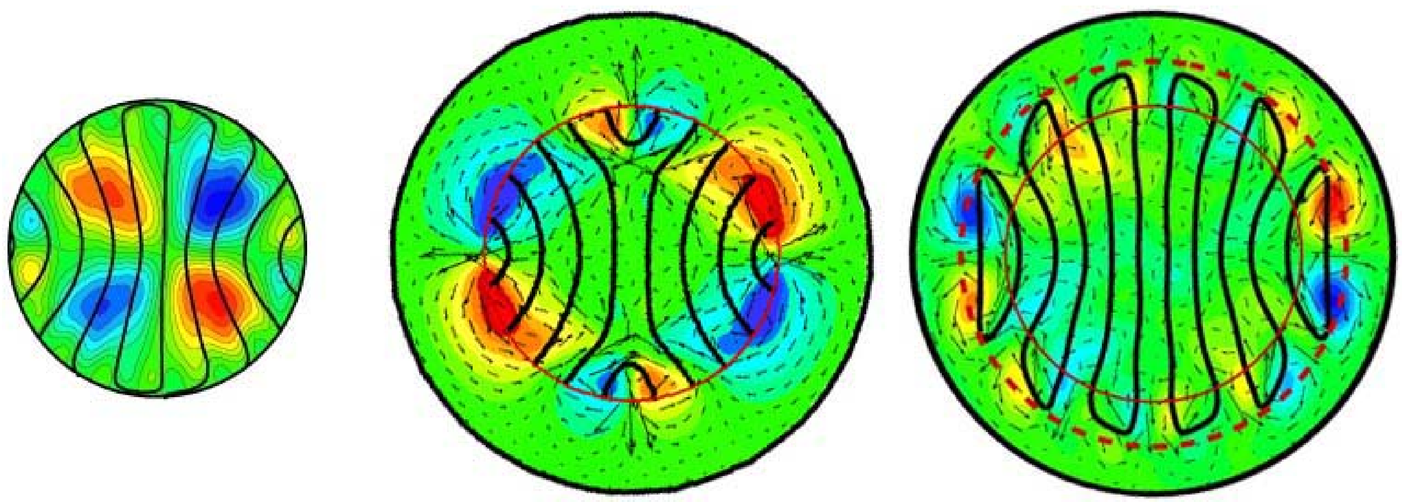

Mean flow

The mean flow, $\vec{U}(x,y)$, can be decomposed as,

$$\vec{U}(x,y) = \vec{U}_d(x,y) + \vec{U}_p(x,y)$$

- The pattern distortion caused by the Reynolds stress term induces a flow $\vec{U}_d(x,y)$.
- For $\vec{U}(x,y)$ to be incompressible a Poiseuille-like flow is generated through a slowly varying pressure, $p_s(x,y)$, the mean of which results in $\vec{U}_p(x,y)$.
- $\vec{U}_p$ is added to $\vec{U}_d$ to yield the divergence free mean flow $\vec{U}(x,y)$.

[See Newell, Passot and Souli in J. Fluid Mech. **220**, 187 (1990) for complete analysis]

Mean flow and spiral defect chaos

$$\sigma^{-1}\left[\frac{\partial\vec{u}}{\partial t}+\left(\vec{u}\bullet\vec{\nabla}\right)\vec{u}\right]=-\vec{\nabla}p+R\,T\hat{e}_z+\nabla^2\vec{u}-\vec{\Phi}$$

$$R=2950,\ \sigma=1,\ t=250$$

Wavenumbers with and without meanflow

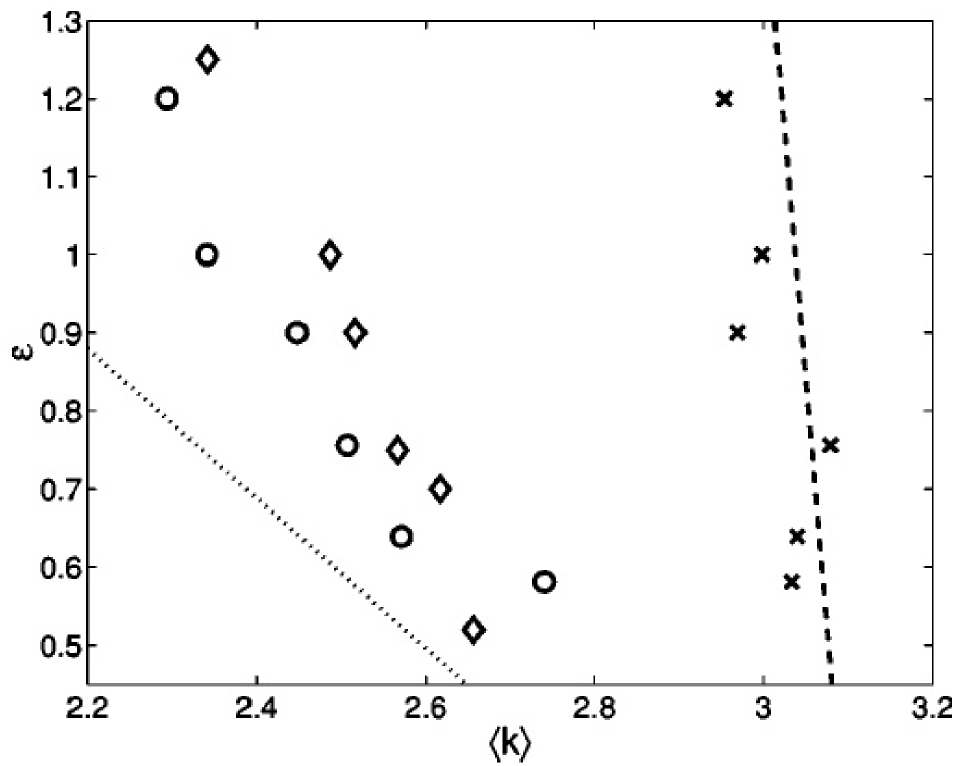

Mean flow and spiral defect chaos

- In the absence of mean flow spiral defect chaos collapses to a stationary state comprised of angular rolls
- The mean wavenumber increases after a quench and approaches the focus selected value (at the zig-zag boundary)
- In the absence of mean flow rolls terminate into lateral walls at an oblique angle

[Chiam, Paul, Cross and Greenside, Phys. Rev. E 67 056206 (2003)]

Pattern coarsening far from equilibrium

Pattern coarsening far from equilibrium

For a system with an ordered stripe state starting from random initial conditions:

What is the long time asymptotic state?
What are the transient dynamics approaching this state?
What disturbance drives the growth of the unstable mode?
How does the length scale over which the stripes grow?
What is the large scale morphology and final selected wavevector?

Transient dynamics

- As the ordered regions get larger the dynamics, which depends on the misalignment between different ordered regions, becomes slower.
- Often (experiment, numerics, theory) a power law dependence is found for a characteristic length of the ordered regions.

$$L(t) \propto t^{\gamma}$$

with $\gamma = 1/2$ common but many others observed. Also logarithmic growth, and power laws with logarithmic corrections.

- Stripe states often show very slow growth e.g. $\gamma = 0.25$.
- The transient dynamics are said to show scaling if different measures of the characteristic length follow the same behavior.

Simulations of Rayleigh-Bénard Convection

- Extended system but aspect ratios are *not* large, $\Gamma \sim 50$ to 100
- Therefore simulation times are not very long before finite size affects the dynamics.
- Our main focus is on the asymptotic state and gross features of transient dynamics (e.g. where $\gamma = 1/4$ or $1/2$ and not whether $\gamma = 1/4$ or $1/5$).

$R = 2169$, $\sigma = 1.4$, and $\Gamma = 57$

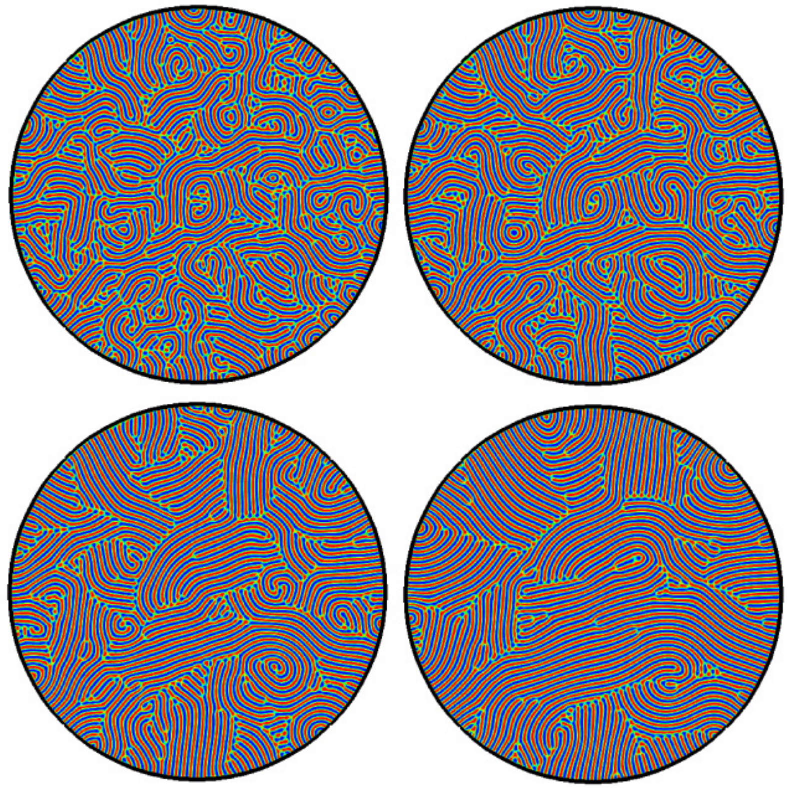

$R = 2169$, $\sigma = 1.4$, $\Gamma = 57$, $t = 16$, 32, 64, and 128

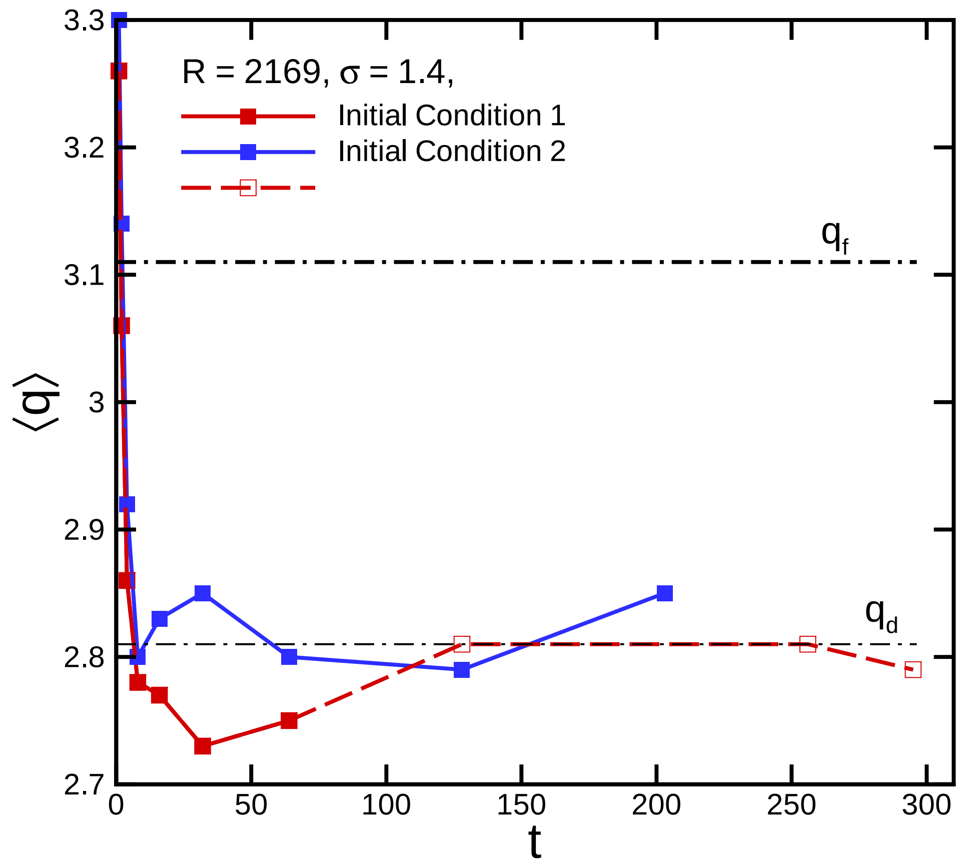

[Exp. ref. for q_d, B.B. Plapp, PhD Thesis, Cornell 1997, Bodenschatz et. al., Ann. Rev. Fluid Mech. **32** 2000]

Domain size: deduced from the width of the Fourier Spectrum

$$S(q) = \left(\frac{a}{(q^2 - b)^2 + c^2} \right)^2, \qquad \delta q = \frac{0.322c}{\sqrt{b}}, \qquad \xi_q \sim \frac{1}{\delta q}$$

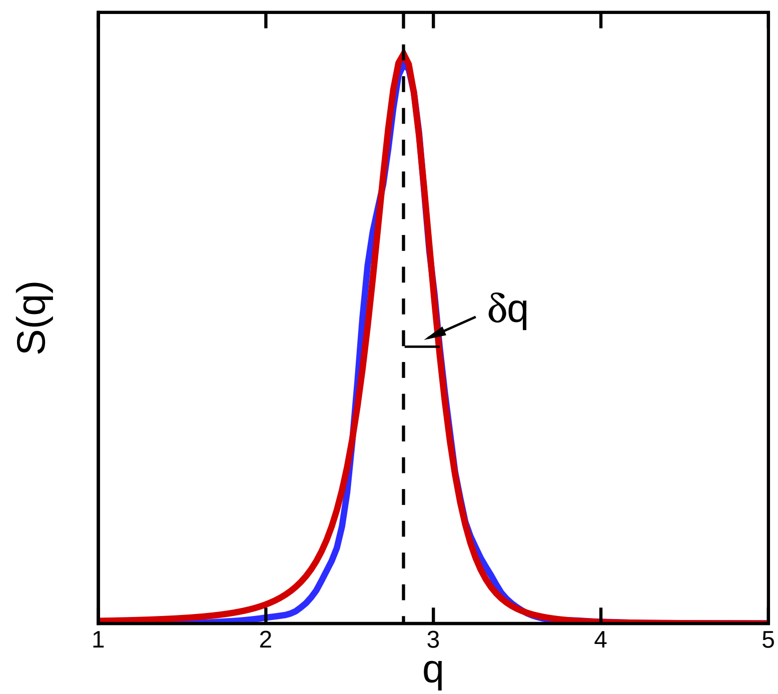

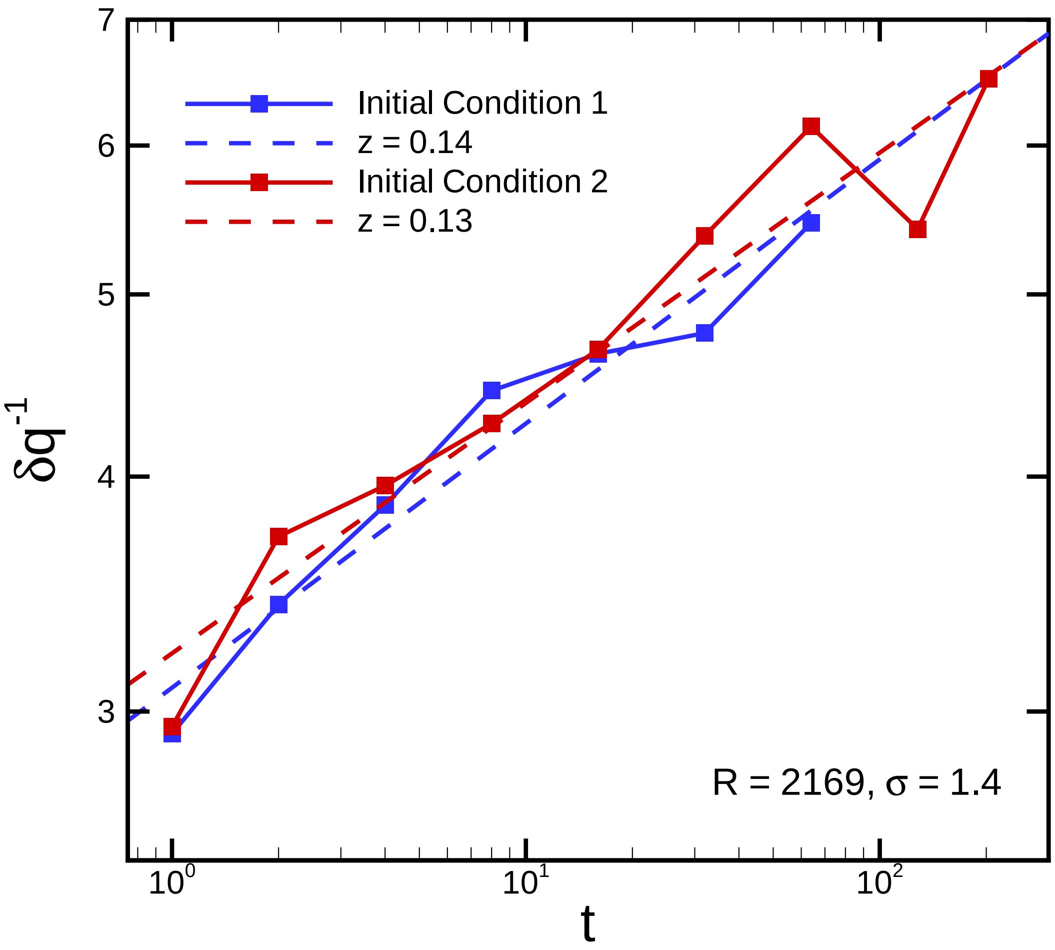

Consistent with small power law $\gamma \sim 0.15$

Orientation field correlation length

$$C_2\left(|\vec{r}-\vec{r'}|,t\right)=\left\langle e^{i2(\theta(\vec{r},t)-\theta(\vec{r'},t))}\right\rangle$$

$$C_2 \sim e^{-r/\xi_o}$$

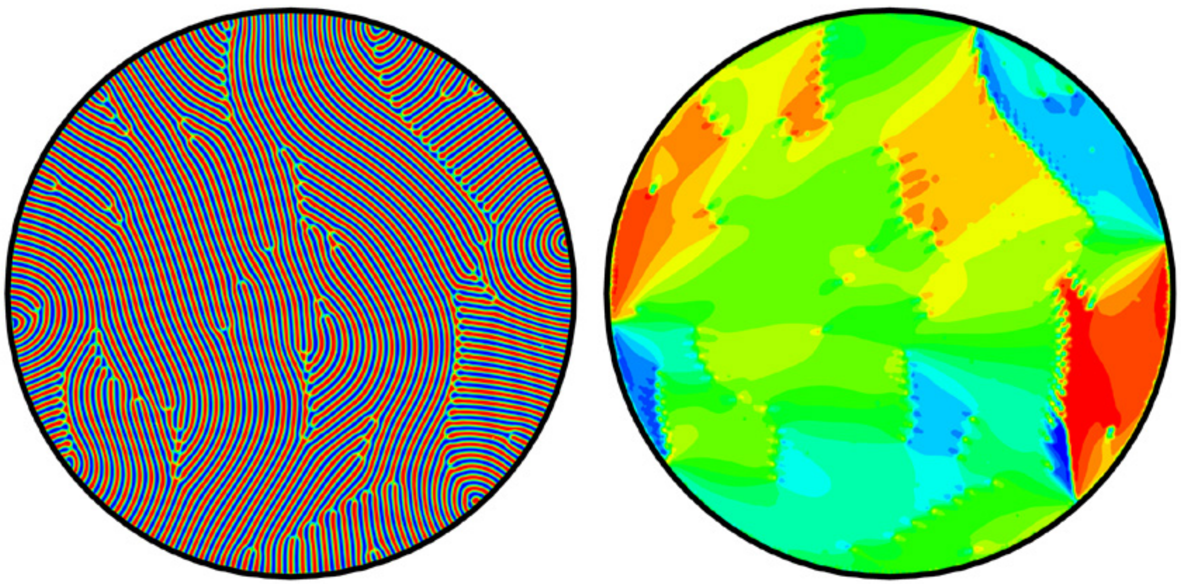

$R=2169$, $\sigma=1.4$, $\Gamma=57$, $t=203$

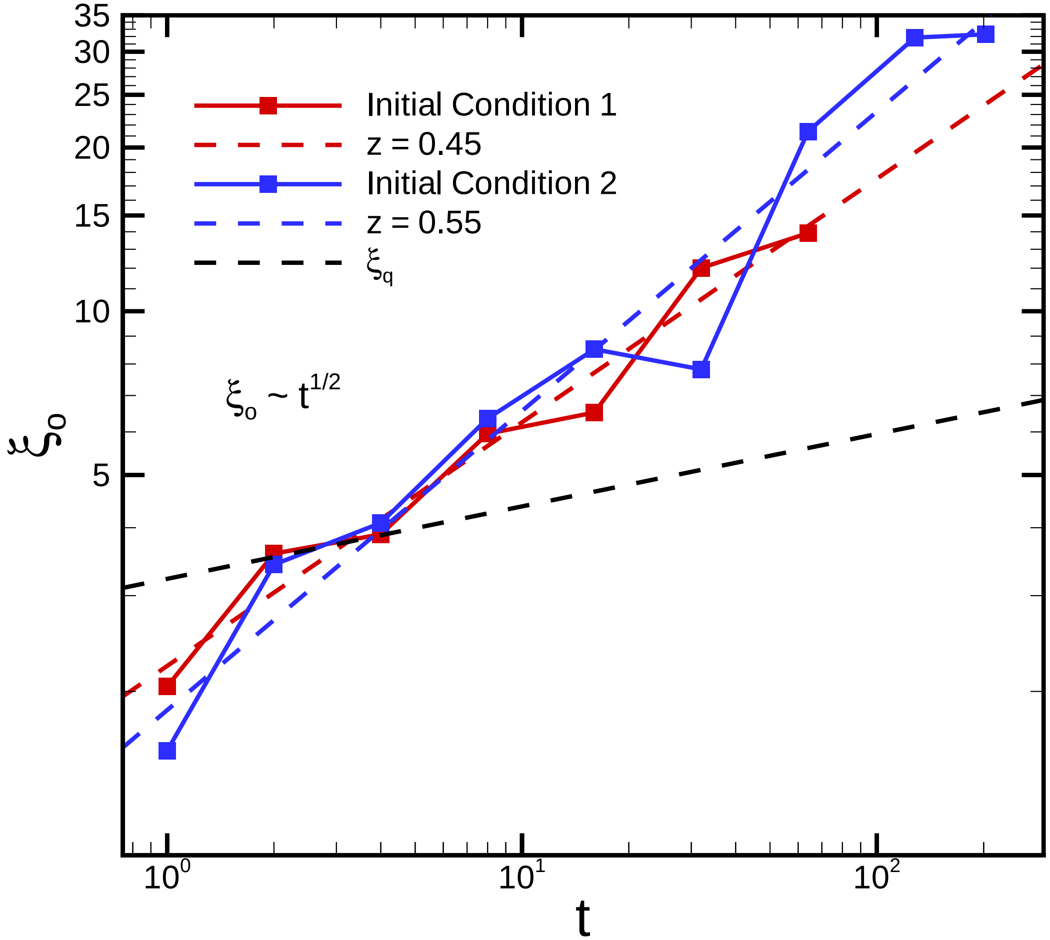

Faster growth $t^{1/2}$

Defect density (defined as regions of large curvature)

Local wavevector, $\vec{k}$

$$|k| \approx \left(\frac{\partial_{xx}\theta}{\theta} \right)^{1/2}$$

Curvature

$$\kappa = \vec{\nabla} \cdot \hat{k}, \qquad \hat{k} = \frac{\vec{k}}{|k|}$$

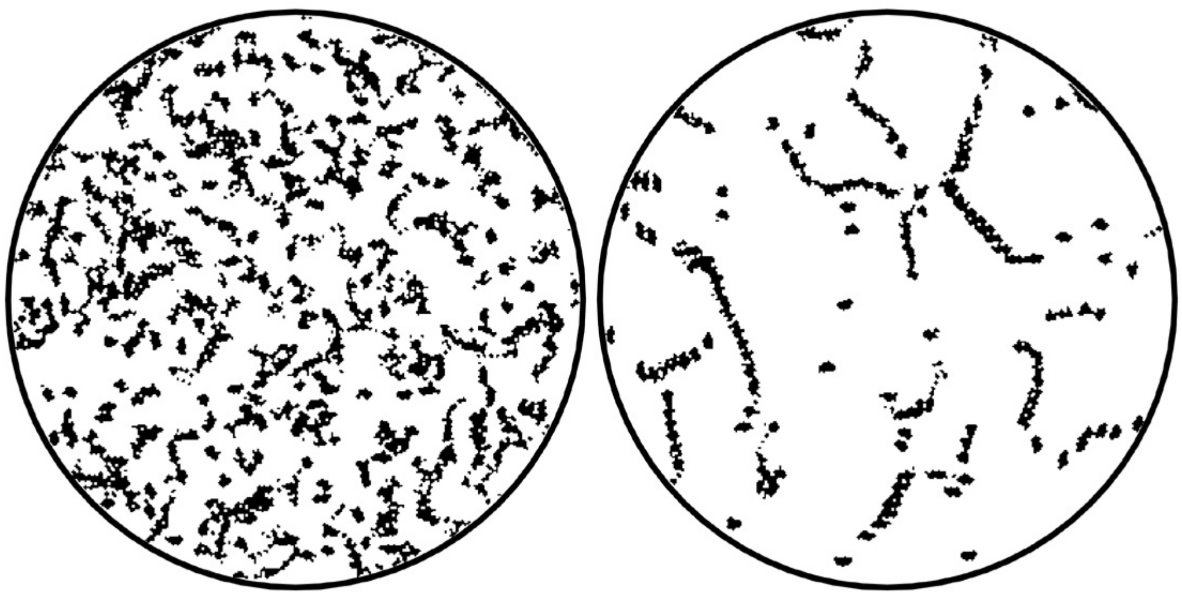

$R = 2169$, $\sigma = 1.4$, $\Gamma = 57$, $t = 8$, 128

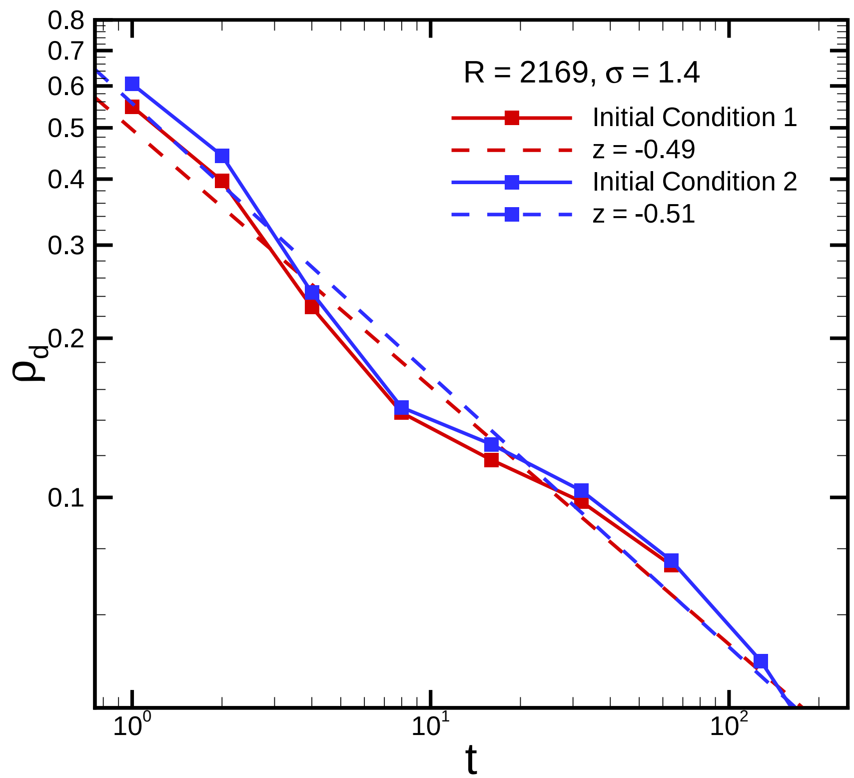

For isolated defects $L_d \sim \rho_d^{-/2}$ so that $L_d \propto t^{1/4}$.

For defect lines ρ_d is the length of a line, and the domain size scales as $t^{1/2}$.

Pattern coarsening far from equilibrium

- Much progress has been made in the equilibrium case
- Coarsening in non-equilibrium systems is very difficult
- Many types of defects: dislocations, disclinations, grain boundaries: hard to identify important dynamical processes
- Simulation data suggests the presence of at least two length scales, $\xi_q \sim t^{0.15}$, $\xi_o \sim t^{1/2}$, $\xi_d \sim t^{1/2}$
- Wavenumber selection in large aspect ratios: patterns evolve toward q_d
- Coarsening experiments in RBC may now be possible ($\Gamma > 100$ for long times – still not reasonable in simulations)
- Will be interesting to study how individual defects interact

Rotating Convection

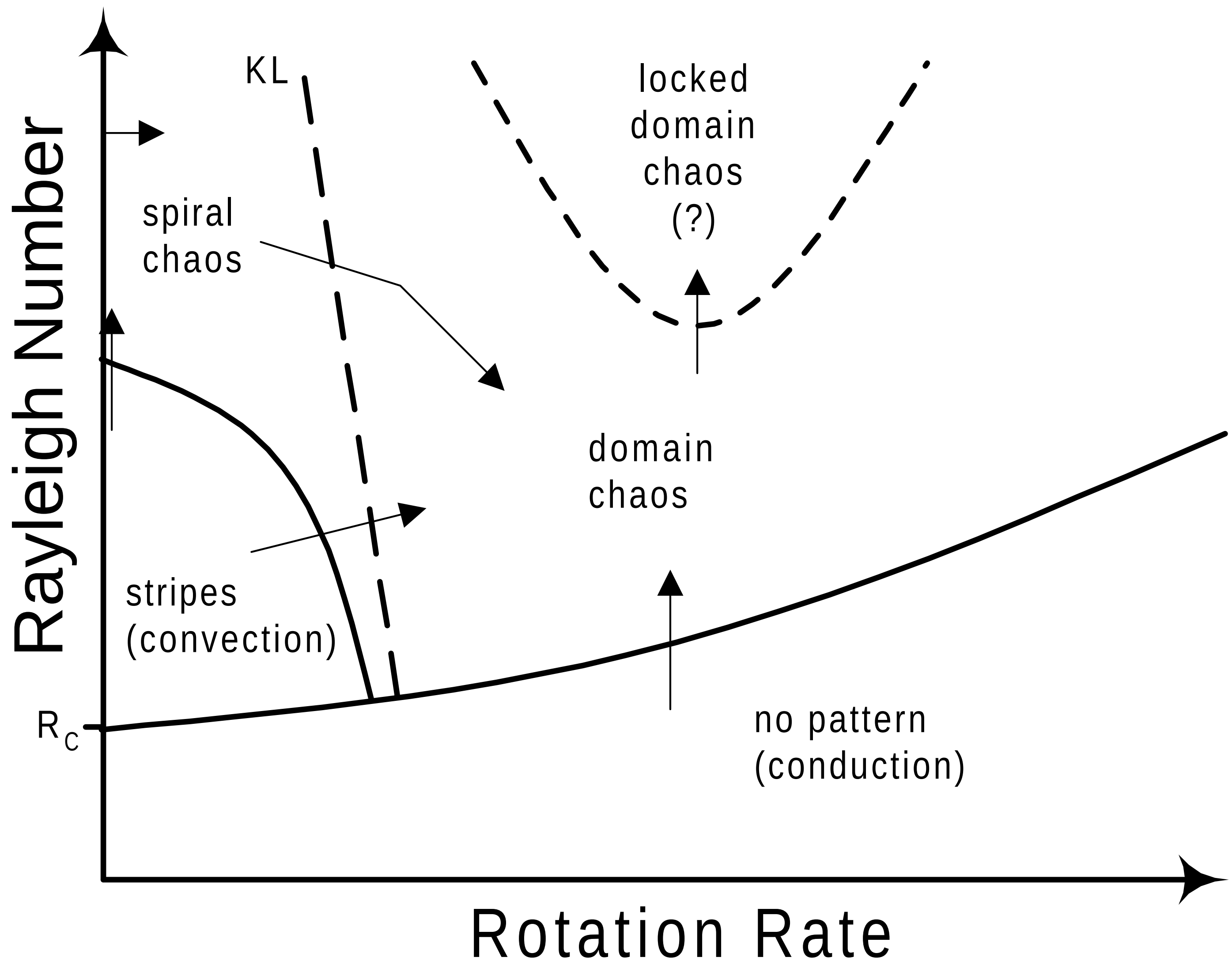
KL
locked
domain
chaos
(?)
spiral
chaos
domain
chaos
stripes
(convection)
no pattern
(conduction)
Rayleigh Number
R_C
Rotation Rate

Domain Chaos

Supercritical bifurcation *directly* to a spatiotemporally chaotic state
This is where one is hopeful to be able to gain theoretical insight – turns out to be not so easy

$$\xi_t \sim \epsilon^{-1/2} \quad \xi_e \sim \epsilon^{-0.2}$$

$$\omega_t \sim \epsilon \quad \omega_e \sim \epsilon^{0.6}$$

What is going on?

1. Finite size effects?
2. Influence of thermal noise?
3. Dislocations nucleating from boundaries, "daggers", "scars" or "birds"
4. Ginzburg-Landau model needs refinement
5. ????

[(t) Tu and Cross, PRL **69** 2515, (e) Hu, Ecke and Ahlers, PRL **74** 5040]

Rotating convection in a finite cylindrical domain

$R = 2400 \ \ (1.07R_c), \Omega = 17.6, \sigma = 0.78$, insulating sidewalls

Rotating convection in a finite cylindrical domain

$R = 2400 \;\; (1.07 R_c), \Omega = 17.6, \sigma = 0.78$, insulating sidewalls

Rotating convection in a periodic box

$R = 2400\ \ (1.07R_c), \Omega = 17.6, \sigma = 0.78$, periodic sidewalls

Similar to unpublished results provided by Werner Pesch

Rotating convection

- Numerical simulations allow the study of aspect ratio dependence (including periodic geometries) and finite size scaling effects
- Numerical simulations allow the study of boundary effects
- The rapid gliding of the “dagger-like” defect structures may play an important role in the dynamics
- It is still very difficult to investigate numerically the scaling laws for large aspect ratio systems with experimentally realistic boundaries

Conclusions

- Numerical simulations of experimentally realistic geometries allow the quantitative link between theory and experiment to be made
- There is a lot to learn from making quantitative comparisons between experiment and theory
- Many interesting questions remain that are now accessible

For more information:

www.cmp.caltech.edu/∼stchaos

www.its.caltech.edu/∼mpaul

mpaul@caltech.edu

General presentation of our progress in numerical simulaion of RBC

Paul, Chiam, Cross, Fischer, and Greenside Physica D **184** 114 (2003)

Chaos in cryogenic liquid Helium

Paul, Cross, Fischer, and Greenside Phys. Rev. Lett. **87** 154501 (2001)

Convection with a radial ramp in plate separation

Paul, Cross and Fischer, Phys. Rev. E **66** 046210 (2002)

Mean flow and spiral defect chaos

Chiam, Paul, Cross and Greenside, Phys. Rev. E **67** 056206 (2003)

Nekton

Fischer, J. Comp. Phys. **133** 84 (1997)

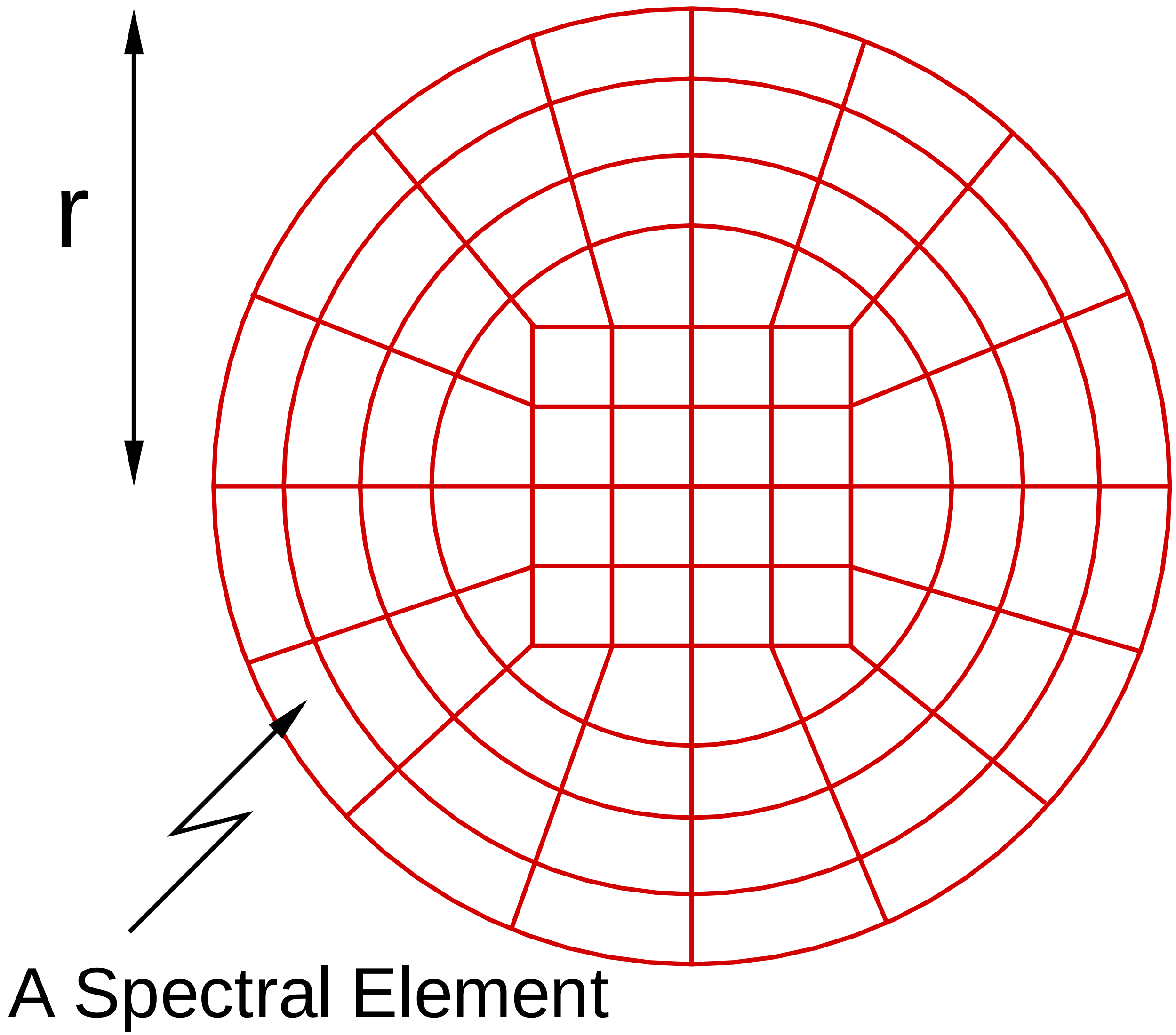
r
A Spectral Element

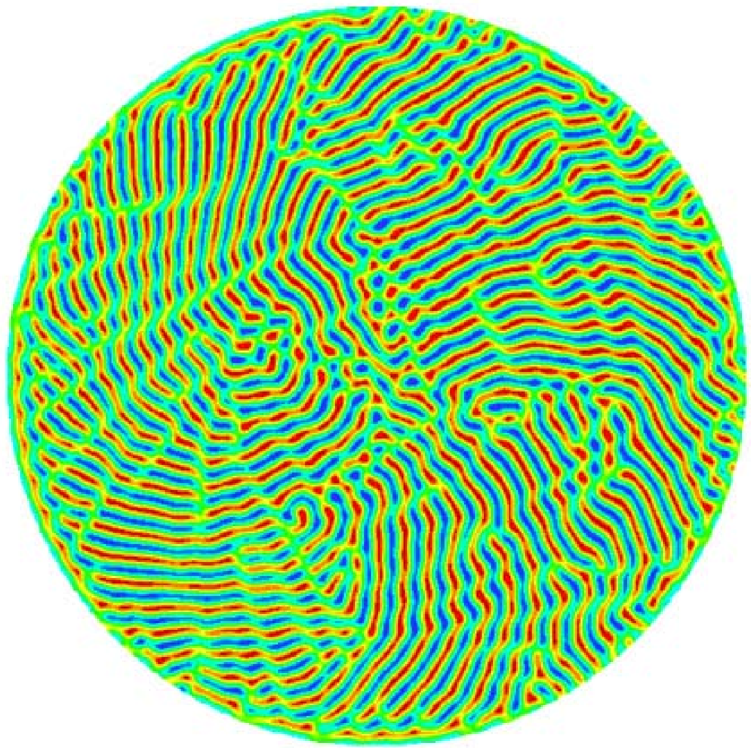

$\Gamma = 30, R = 3200, \sigma = 1.0, \Omega = 17.6$, Insulating sidewalls

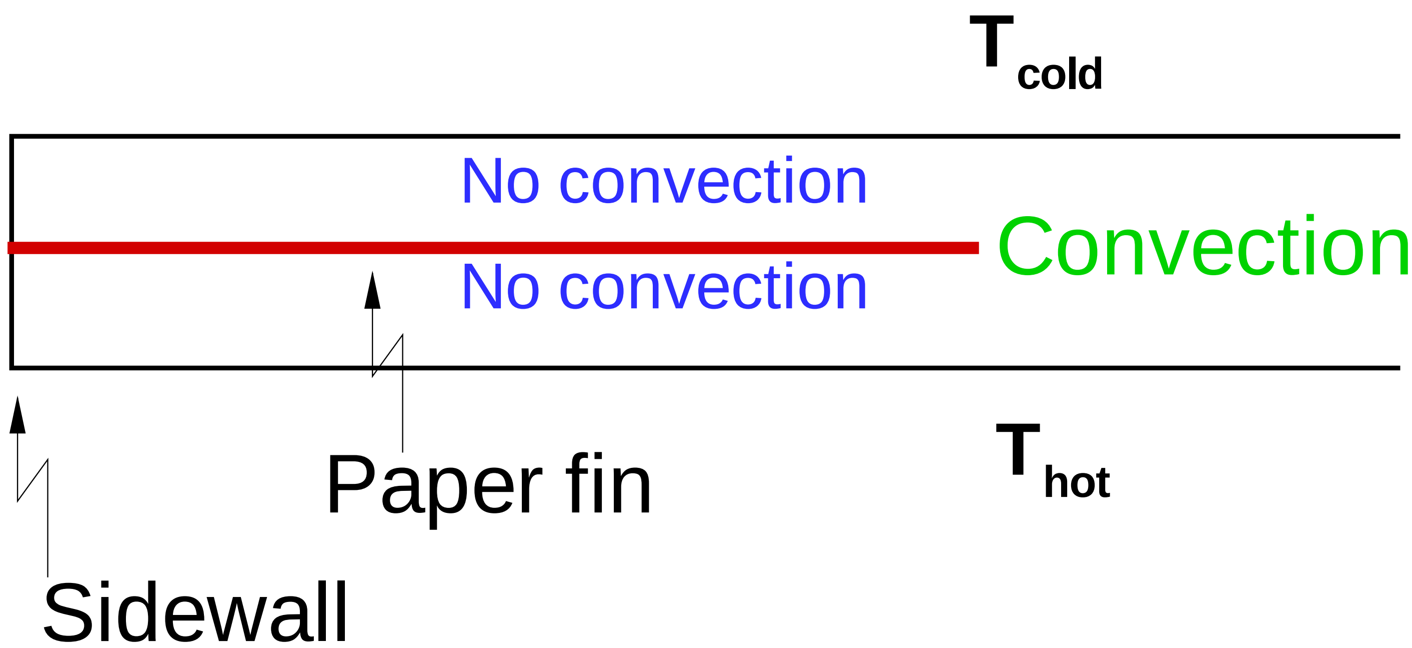

Paper fin is a no slip surface
and inhibits convection.

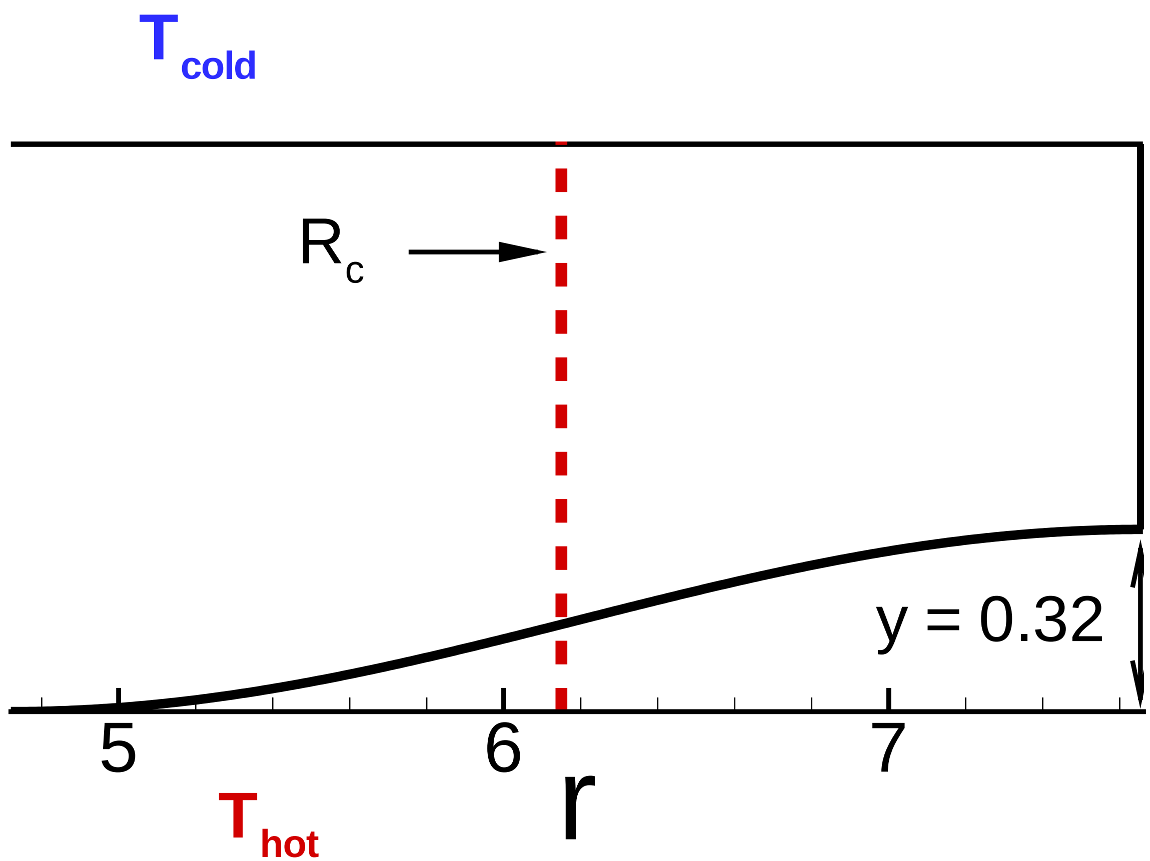
T_{cold}
R_c
y = 0.32
5
6
7
r
T_{hot}

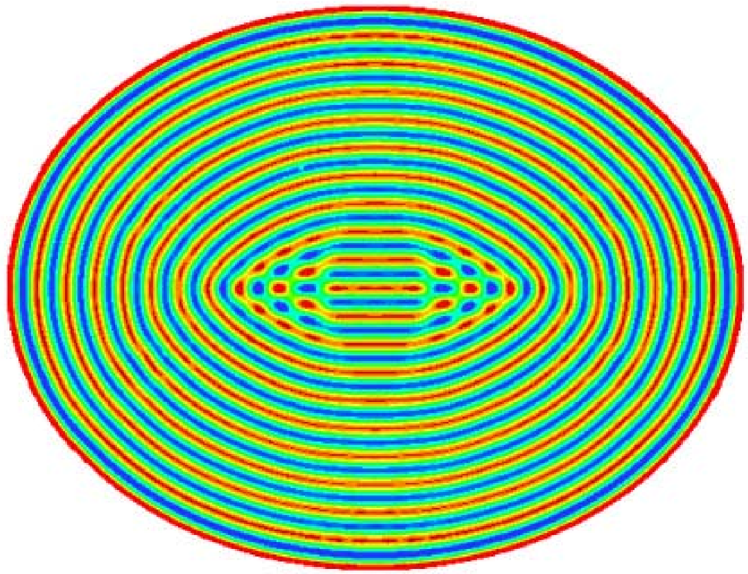

$R = 2000, \sigma = 100, t = 40\tau_v$, Hot sidewall

$a = 26, b = 20, e = 0.639$

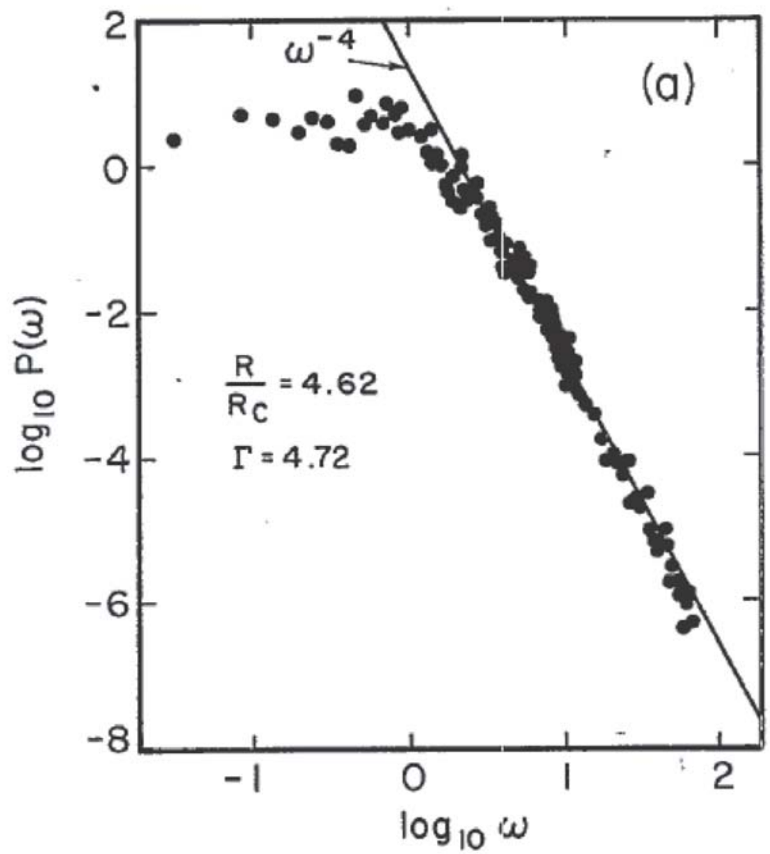

G. Ahlers and R. P. Behringer, Phys. Rev. Lett. **40**, 712 (1978)

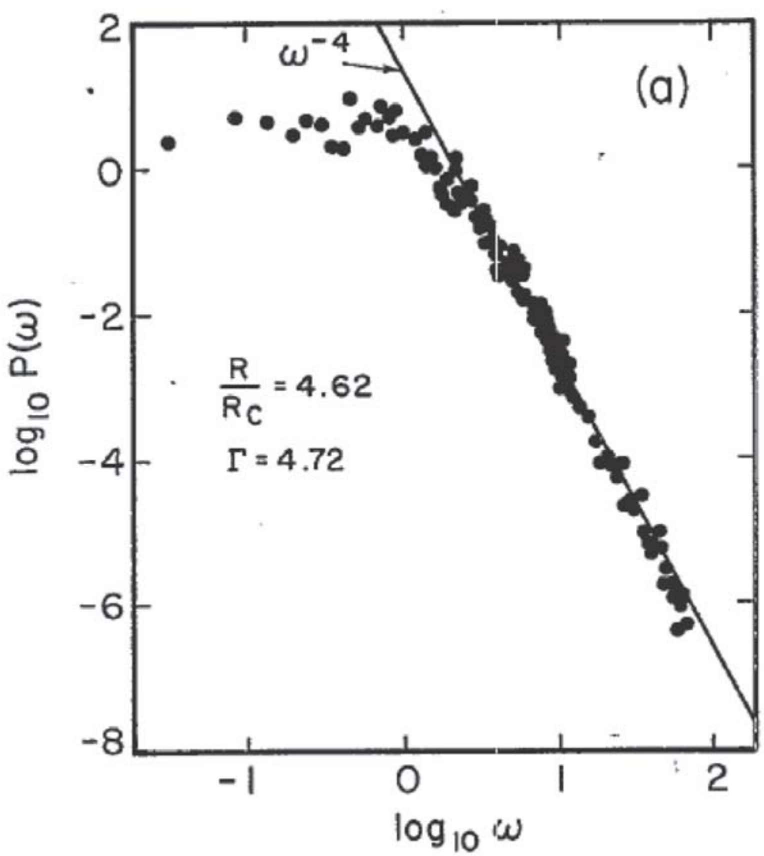

ω^{-4}
(a)
$\frac{R}{R_C} = 4.62$
$\Gamma = 4.72$
$\log_{10} P(\omega)$
$\log_{10} \omega$

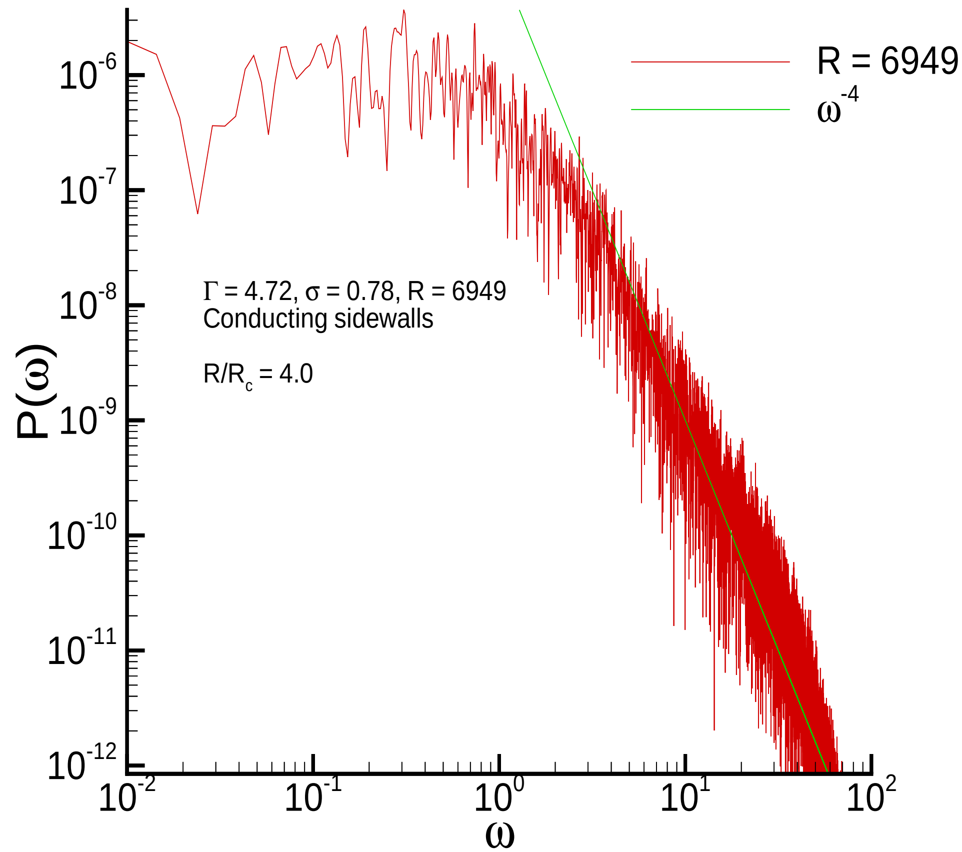

R = 6949
ω^{-4}
$\Gamma = 4.72$, $\sigma = 0.78$, R = 6949
Conducting sidewalls
$R/R_c = 4.0$
$P(\omega)$
ω

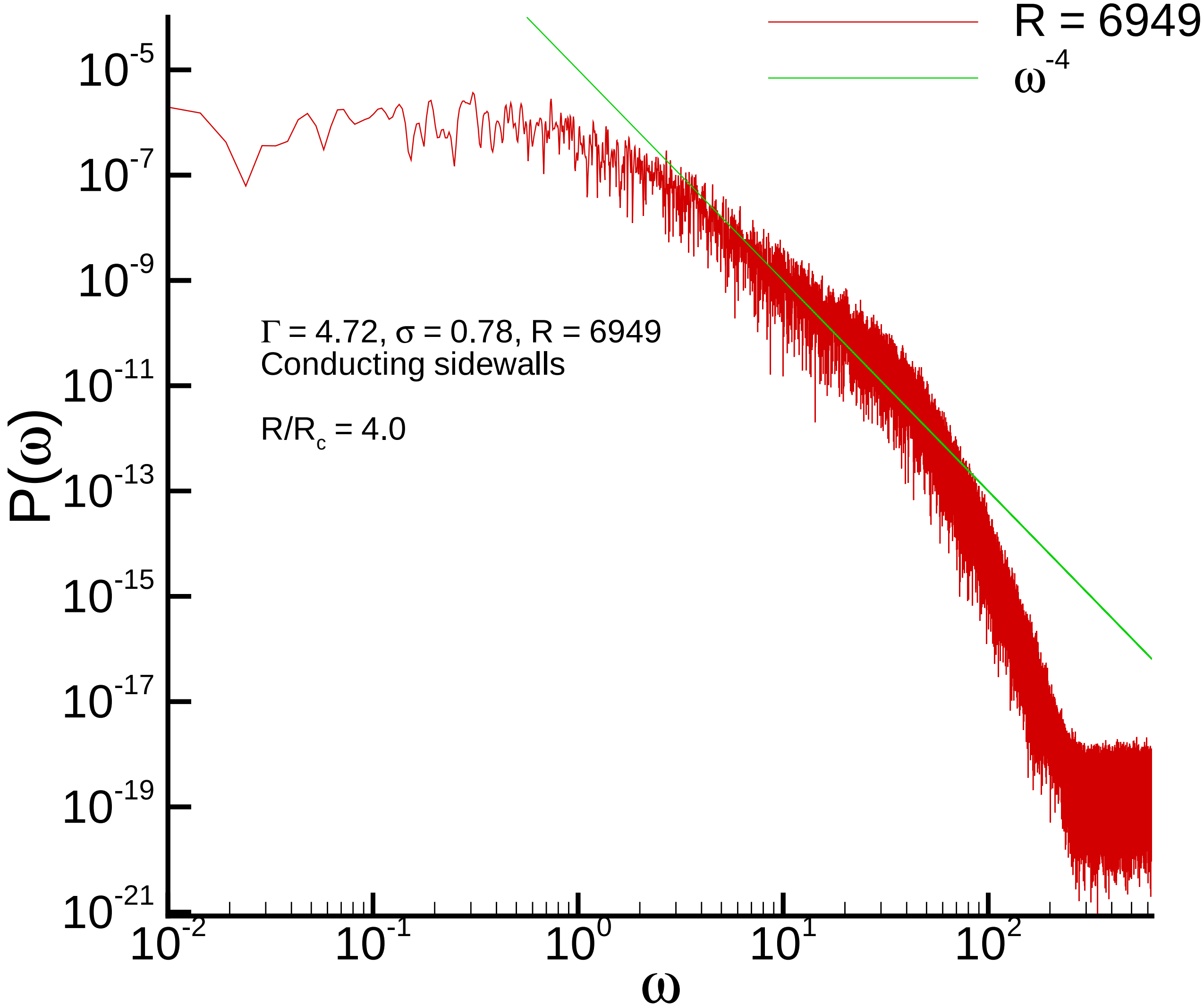
R = 6949
ω^-4
10^-5
10^-7
10^-9
10^-11
10^-13
10^-15
10^-17
10^-19
10^-21
P(ω)
Γ = 4.72, σ = 0.78, R = 6949
Conducting sidewalls
R/R_c = 4.0
10^-2
10^-1
10^0
10^1
10^2
ω

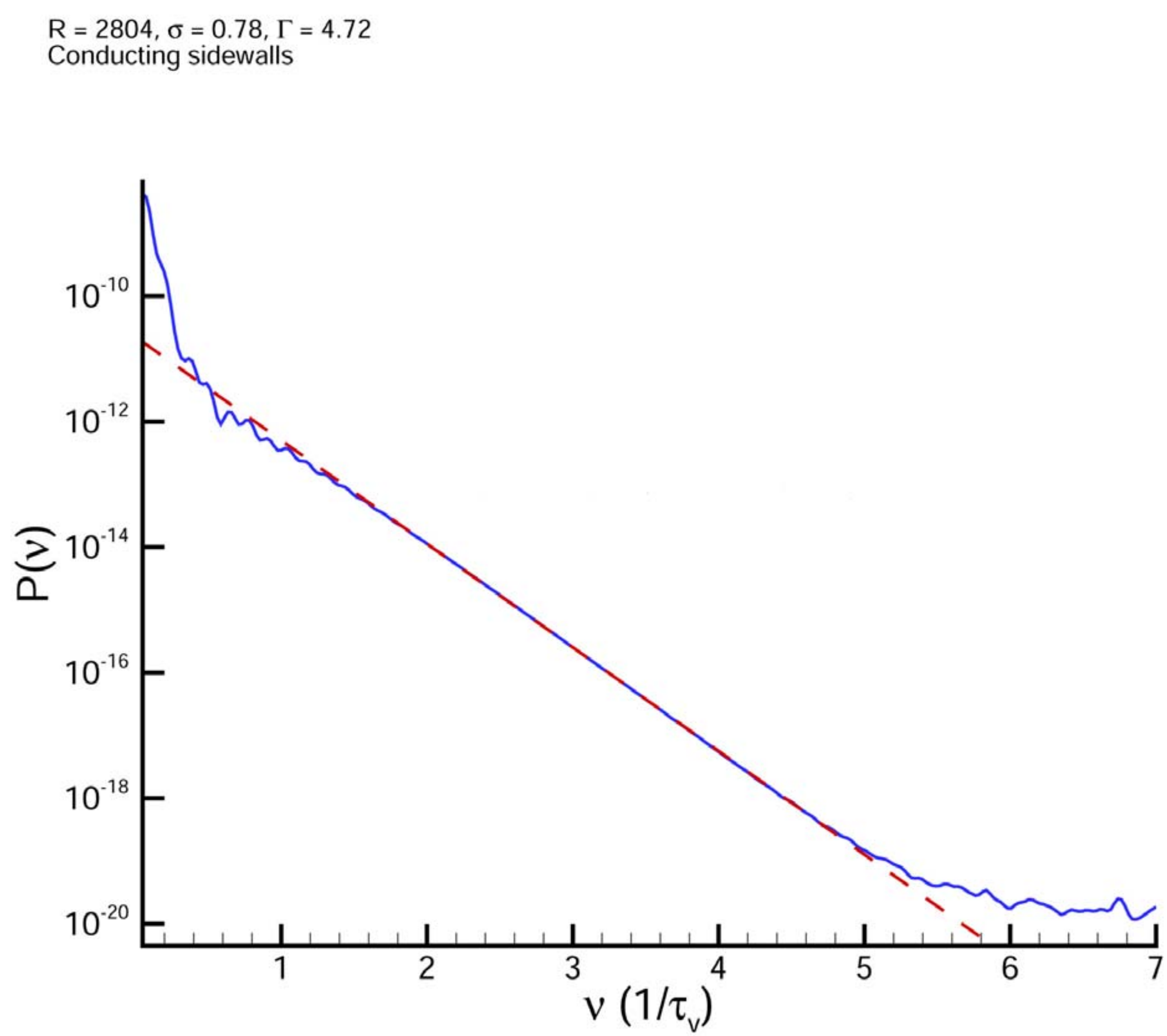
R = 2804, σ = 0.78, Γ = 4.72
Conducting sidewalls
P(ν)
10^-10
10^-12
10^-14
10^-16
10^-18
10^-20
1
2
3
4
5
6
7
ν (1/τ_v)

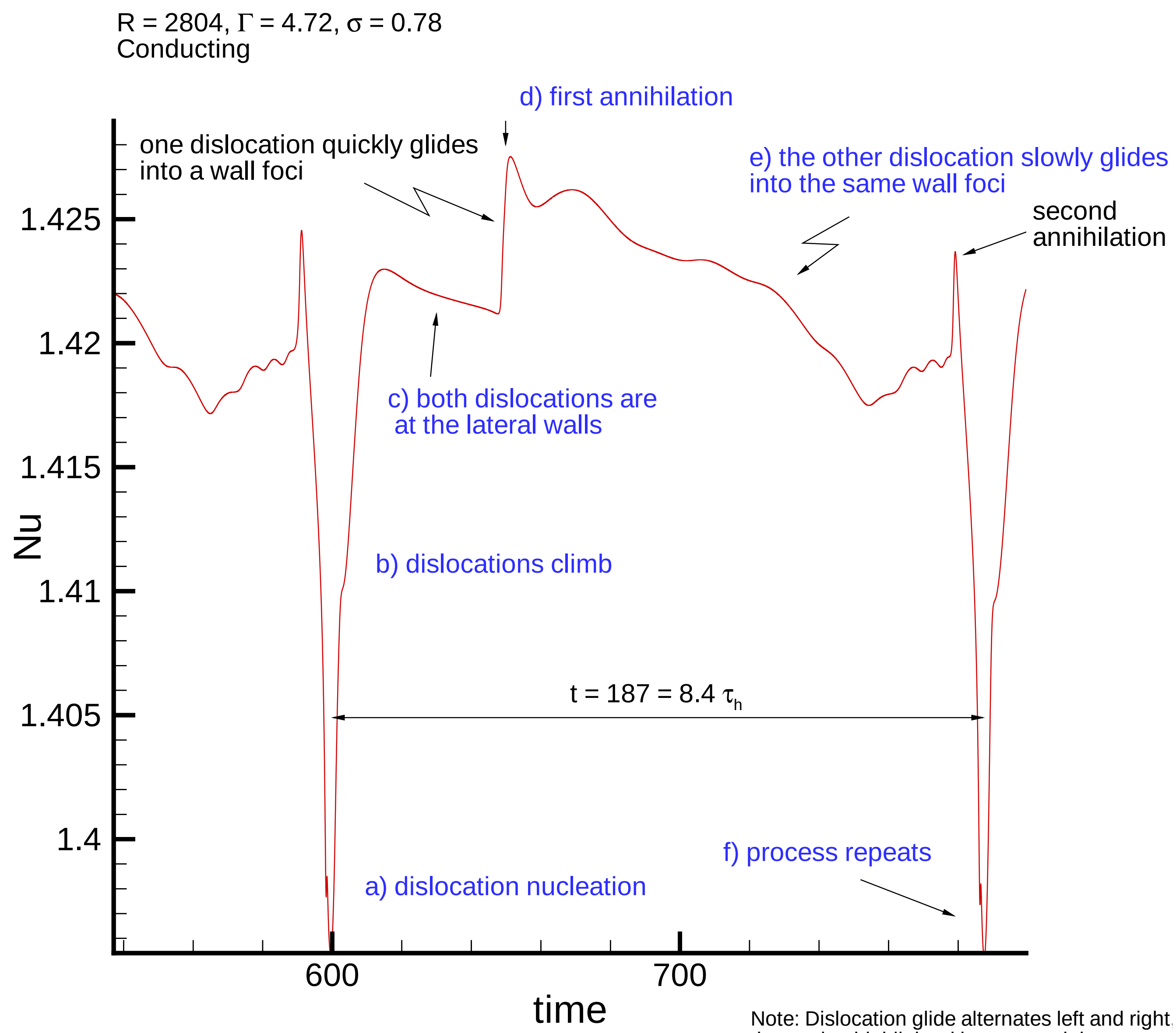

Note: Dislocation glide alternates left and right, the portion highlighted here goes right.